

# High-Yield Synthesis of the Enterobactin Trilactone and Evaluation of Derivative Siderophore Analogs<sup>1</sup>

Michel Meyer,<sup>†</sup> Jason R. Telford, Seth M. Cohen, David J. White, Jide Xu, and Kenneth N. Raymond\*

Contribution from the Department of Chemistry, University of California, Berkeley, California 94720

Received March 6, 1997<sup>⊗</sup>

**Abstract:** A novel one-step synthesis of the macrocyclic triserine trilactone scaffold of the siderophore enterobactin, which eliminates the  $\beta$ -lactonization step of *N*-tritylserine, is presented. The cyclization reaction is based on a stannoxane template and leads to an overall yield of  $\sim 50\%$ . This enables the practical functionalization of the trilactone by attaching chelating groups other than catecholamides. The conformational stability of the trilactone ring has been examined by high-resolution X-ray diffraction studies of the *N*-trityl intermediate: crystals grown from methylene chloride:methanol are orthorhombic, space group  $P2_12_12_1$  with unit cell dimensions  $a = 9.2495(5)$  Å,  $b = 11.3584(1)$  Å,  $c = 48.945(1)$  Å,  $V = 5142.1(2)$  Å<sup>3</sup>, and  $Z = 4$ . A hydroxypyridinonate analog of enterobactin, *N,N',N''*-tris[(3-hydroxy-1-methyl-2-oxo-(1*H*-pyridinyl)carbonyl]-4-cyclotrisceryl trilactone (hopobactin), has been prepared by attachment of three 3-hydroxy-1-methyl-2-(1*H*)-pyridinonate (3,2-HOPO) moieties to the triserine trilactone. This ligand represents the first enterobactin analog that retains the trilactone scaffold, but employs chelates other than catecholamides. Crystals of the chiral ferric complex grown from DMF:diethyl ether are monoclinic, space group  $P2_1$ , with unit cell dimensions  $a = 13.0366(9)$  Å,  $b = 22.632(2)$  Å,  $c = 27.130(2)$  Å,  $V = 100.926(1)^\circ$ ,  $V = 7860(1)$  Å<sup>3</sup>, and  $Z = 8$ . The  $\Delta$  configuration of enterobactin metal complexes is also enforced in those of hopobactin and persists in aqueous or methanolic solution, as demonstrated by circular dichroism. The ferric hopobactin complex is the first reported chiral complex of hydroxypyridinonate ligands. The solution coordination chemistry of this new ligand and its iron(III) and iron(II) complexes have been studied by means of <sup>1</sup>H NMR, potentiometric, spectrophotometric, and voltammetric methods. The average protonation constant of the hopobactin free ligand ( $\log K_{av} = 6.1$ ) is typical of other 3-hydroxy-1-methyl-2-oxo-1*H*-pyridin-4-carboxamide ligands. The stability constants of the iron(III) complex formed with hopobactin ( $\log \beta_{110} = 26.4$ ) and with the tris(2-aminoethyl)amine-based analog, TRENHOPO, ( $\log \beta_{110} = 26.7$ ) are of the same order of magnitude, unlike the catecholamide-based species, where enterobactin ( $\log \beta_{110} = 49$ ) is 6 orders of magnitude more stable than TRENAM ( $\log \beta_{110} = 43.6$ ). The stability enhancement reflects the specific predisposition by the triserine scaffold of the catecholamide binding units. In spite of a significantly lower affinity of 3,2-hydroxypyridinonates for iron(III) compared with the more basic catecholates, hopobactin is an extraordinarily powerful chelating agent under acidic conditions: No measurable dissociation is observed even in 1.0 M HCl. In contrast to enterobactin and its synthetic derivatives, the hopobactin ferric complex undergoes no sequential protonation above pH 1. The affinity of hopobactin and TRENHOPO for iron(III) relative to iron(II) results in strongly negative reduction potentials,  $-782$  mV vs 0.01 M Ag<sup>+</sup>/Ag in CH<sub>3</sub>CN or  $-342$  mV vs NHE in water and  $-875$  mV vs 0.01 M Ag<sup>+</sup>/Ag in CH<sub>3</sub>CN or  $-435$  mV vs NHE in water, respectively.

## Introduction

Of the nutrients required by bacteria and fungi for growth, one of the most difficult to obtain is iron. The hydrolysis of Fe(III) limits its concentration at neutral pH to about  $10^{-18}$  M, requiring organisms to develop some form of complexation and active transport. To this end microbes (and in some cases plants) produce low-molecular weight chelating agents, siderophores.<sup>2–5</sup> Novel features of siderophore-mediated iron transport by aerobic bacteria involve energy-dependent transport across cell membranes (including the outer membrane of Gram-

negative bacteria) and recognition of the iron–siderophore complex based on the chirality of the octahedral metal center.<sup>6,7</sup> Because the growth of pathogenic bacteria is dependent on iron availability, iron metabolism has increasingly been recognized as significant to medicine as a determinant in bacterial disease.<sup>8–13</sup>

Isolated over 20 years ago,<sup>14,15</sup> enterobactin is one of the best characterized siderophores with respect to the mechanism and genetics of its cellular transport and production.<sup>16–18</sup> Entero-

(6) Müller, G.; Matzanke, B. F.; Raymond, K. N. *J. Bacteriol.* **1984**, *160*, 313.

(7) Matzanke, B. F.; Müller-Matzanke, G.; Raymond, K. N. Siderophore Mediated Iron Transport. In *Physical Bioinorganic Chemistry Series*; Loehr, T. M., Ed.; VCH: New York, 1989; p 1.

(8) Holbein, B. E.; Jericho, K. W. F.; Likes, G. C. *Infect. Immun.* **1979**, *24*, 545.

(9) Bullen, J. J.; Leigh, L. C.; Rogers, H. J. *Immunology* **1968**, *15*, 581.

(10) Expert, D.; Gill, P. R. *Iron: A Modulator in Bacterial Virulence and Symbiotic Nitrogen-Fixation*; CRC Press: Boca Raton, 1992.

(11) Martínez, J. L.; Delgado-Iribarren, A.; Baquero, F. *FEMS Microbiol. Rev.* **1990**, *75*, 45.

(12) Tai, S.-P. S.; Krafft, A. E.; Nootheti, P.; Holmes, R. K. *Microb. Pathogen.* **1990**, *9*, 267.

(13) Griffiths, E. *Biol. Met.* **1991**, *4*, 7.

(14) O'Brien, J. G.; Gibson, F. *Biochim. Biophys. Acta* **1970**, *215*, 393.

(15) Pollack, J. R.; Neilands, J. B. *Biochem. Biophys. Res. Commun.* **1970**, *38*, 989.

\* Author to whom correspondence should be addressed.

<sup>†</sup>Present address: Laboratoire d'Ingénierie Moléculaire pour la Séparation et les Applications des Gaz (LIMSAG), UMR 5633, Université de Bourgogne, Dijon, France.

<sup>⊗</sup> Abstract published in *Advance ACS Abstracts*, October 1, 1997.

(1) Coordination Chemistry of Microbial Iron Transport. 60. For the previous paper in this series, see: Kersting, B.; Meyer, M.; Powers, R. E.; Raymond, K. N. *J. Am. Chem. Soc.* **1996**, *118*, 7221.

(2) Winkelmann, G. *CRC Handbook of Microbial Iron Chelates*; CRC Press: Boca Raton, 1991.

(3) Winkelmann, G. *Mycol. Res.* **1992**, *96*, 529.

(4) Neilands, J. B. *J. Biol. Chem.* **1995**, *270*, 26723.

(5) Telford, J. R.; Raymond, K. N. Siderophores. In *Comprehensive Supramolecular Chemistry*; Atwood, J. L., Davies, J. E. D., MacNicol, D. D., Vögtle, F., Eds.; Elsevier Science Ltd.: Oxford, 1996; Vol. 1; p 245.

bactin forms a remarkably stable complex with iron<sup>19</sup> and is the primary siderophore of enteric bacteria. (Although a triphenolate derivative of 1,4,7 triazacyclononane has been reported to have a higher stability constant,<sup>20a</sup> this ligand is insoluble in water. The results in 75% ethanol/25% H<sub>2</sub>O solution cannot be directly compared with aqueous solution. However a related hydroxypyridyl derivative is reported to bind Fe<sup>3+</sup> more strongly than enterobactin at neutral pH<sup>20b</sup>.) These features have prompted a range of studies of enterobactin's coordination chemistry and the structural origins of its unusual stability.<sup>21–28</sup> Synthetic enterobactin mimics have been hexadentate triscatecholamide ligands coupled to a variety of triamine scaffolds including carbocycles,<sup>29,30</sup> tripodal<sup>31,32</sup> or cyclic<sup>32,33</sup> polyamines, mesityl,<sup>32–35</sup> and *scyllo*-inositol<sup>36</sup> derivatives. Most of these analogs form Fe(III) complexes about 10<sup>6</sup> less stable than that of enterobactin.

Recently, the origin of this enhanced stability has been attributed to the positioning of the ligand groups by the trilactone ring of enterobactin.<sup>35,37</sup> This rigid scaffold imposes a  $\Delta$  stereochemistry on the high-spin Fe(III) metal center.<sup>23</sup> However, the difficulty of synthesizing the 12-membered trilactone ring has been a major barrier to the preparation of enterobactin analogs based on the same trilactone scaffold. The first syntheses gave overall yields from multistep reactions of only about 1%.<sup>38–40</sup> The organotin template strategy developed by Shanzer et al. increased the yield to about 6%.<sup>41</sup> Recently, Gutierrez et al. improved the multistep Shanzer synthesis to give practical yields.<sup>42</sup>

This paper presents a novel, one-step synthesis of the enterobactin scaffold in yields as high as 50%. This high-yield synthesis enables the preparation of new synthetic analogs of

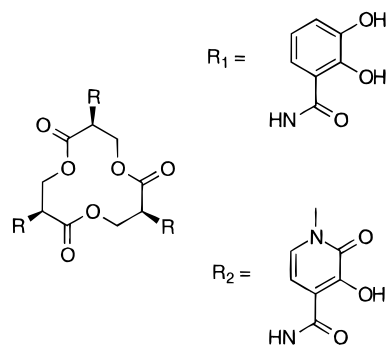


**Figure 1.** The natural siderophore enterobactin ( $R_1$  = catechol) and its synthetic 3,2-hydroxypyridinonate analog hopobactin ( $R_2$  = 3,2-HOPO).

enterobactin that retain the trilactone ring. For the first time, the predisposition ability of the enterobactin scaffold has been gauged with chelates other than catecholamides. To this end, a novel ligand, *N,N',N''*-tris[3-hydroxy-1-methyl-2-oxo-1*H*-pyridin-4-yl]carbonyl]cyclotriseryl trilactone, named here hopobactin (Figure 1), has been synthesized by attaching 3-hydroxy-1-methyl-2(1*H*)-pyridinonate (3,2-HOPO) binding groups to the trilactone triamine. The X-ray structure of ferric hopobactin along with the spectroscopic and thermodynamic properties of this novel ligand and its iron(III) complex have been fully investigated.

## Experimental Section

**General.** Unless otherwise noted, starting materials were obtained from commercial suppliers and used without further purification. Solvents were distilled prior to use. HCl in dry ethanol was prepared by passing dry HCl gas through absolute ethanol, previously distilled over CaH<sub>2</sub>. The concentration was estimated by weight difference and measured by titrating an aliquot (1.0–2.0 mL) of the solution with standardized base. Flash silica gel chromatography was performed using Merck 40–70 mesh silica gel. Radial chromatography was performed on a Chromatotron (Harrison Research) with silica-coated disks. Microanalyses were performed by the Microanalytical Services Laboratory, College of Chemistry, University of California, Berkeley, CA. Mass spectra were recorded at the Mass Spectrometry Laboratory, College of Chemistry, University of California, Berkeley, CA. <sup>1</sup>H NMR spectra were recorded on either AMX 300, AMX 400, or AM 500 Bruker superconducting Fourier-transform spectrometers operating at 300, 400, and 500 MHz, respectively. Infrared spectra were measured using a Nicolet Magna IR 550 Fourier-transform spectrometer. Melting points were taken on a Büchi melting apparatus and are uncorrected. Circular dichroism spectra were recorded using a quartz cell of 1 cm optical path length (Hellma, Suprasil) on a Jasco J500C spectrometer which was equipped with an IF-500 II A/D converter and controlled by a microcomputer.

**Syntheses.** **1,1,6,6-Tetra-*n*-butyl-1,6-distanna-2,5,7,10-tetraoxacyclodecane, Stannoxane (1).** Dibutyltin oxide (100 g, 0.4 mol), ethylene glycol (25 g, 0.4 mol), and benzene (1 L) were added to a flask fitted with a condenser and a Dean–Stark trap. The reaction mixture was refluxed overnight, collecting about 5 mL of liquid in the trap. The solution was cooled to 4 °C whereupon white crystals formed. These were collected by filtration, washed with benzene, and dried. Yield: 90%. Mp: 222–224 °C (lit. mp 223–227 °C).<sup>43</sup> FT IR (thin film cast from CHCl<sub>3</sub>):  $\nu$  2900, 1420, 1050, 910, 590 cm<sup>-1</sup> (no evidence for hydroxyl absorption). <sup>1</sup>H NMR (500 MHz, CDCl<sub>3</sub>):  $\delta$  0.87 (t,  $J$  = 2.92 Hz, 12H), 1.25 (br t,  $J$  = 3.2 Hz, 8H), 1.34 (m,  $J$  = 2.94 Hz,  $J'$  = 2.92 Hz, 8H), 1.6 (m,  $J$  = 3.2 Hz,  $J'$  = 2.94 Hz, 8H), 3.57 (s,

(16) Ecker, D. J.; Matzanke, B. F.; Raymond, K. N. *J. Bacteriol.* **1986**, *167*, 666.

(17) Raymond, K. N.; Cass, M. E.; Evans, S. L. *Pure Appl. Chem.* **1987**, *59*, 771.

(18) Poole, K.; Young, L.; Neshat, S. *J. Bacteriol.* **1990**, *172*, 6991.

(19) Loomis, L. D.; Raymond, K. N. *Inorg. Chem.* **1991**, *30*, 906.

(20) (a) Clarke, E. T.; Martell, A. E. *Inorg. Chim. Acta* **1991**, *186*, 103. (b) Motekaitis, R. J.; Sun, Y.; Martell, A. E. *Inorg. Chim. Acta* **1992**, *198*, 421.

(21) Isied, S. S.; Kuo, G.; Raymond, K. N. *J. Am. Chem. Soc.* **1976**, *98*, 1763.

(22) Salama, S.; Stong, J. D.; Neilands, J. B.; Spiro, T. G. *Biochemistry* **1978**, *17*, 3781.

(23) McArdle, J. V.; Sofen, S. R.; Cooper, S. R.; Raymond, K. N. *Inorg. Chem.* **1978**, *17*, 3075.

(24) Harris, W. R.; Carrano, C. J.; Raymond, K. N. *J. Am. Chem. Soc.* **1979**, *101*, 2722.

(25) Lee, C.-W.; Ecker, D. J.; Raymond, K. N. *J. Am. Chem. Soc.* **1985**, *107*, 6920.

(26) Scarrow, R. C.; Ecker, D. J.; Ng, C.; Liu, S.; Raymond, K. N. *Inorg. Chem.* **1991**, *30*, 900.

(27) Tor, Y.; Libman, J.; Shanzer, A.; Felder, C. E.; Lifson, S. *J. Am. Chem. Soc.* **1992**, *114*, 6661.

(28) Karpishin, T. B.; Raymond, K. N. *Angew. Chem., Int. Ed. Engl.* **1992**, *31*, 466.

(29) Corey, E. J.; Hurt, S. D. *Tetrahedron Lett.* **1977**, *45*, 3923.

(30) Tse, B.; Kishi, Y. *J. Org. Chem.* **1994**, *59*, 7807.

(31) Rodgers, S. J.; Lee, C.-W.; Ng, C. Y.; Raymond, K. N. *Inorg. Chem.* **1987**, *26*, 1622.

(32) Harris, W. R.; Raymond, K. N.; Weilt, F. L. *J. Am. Chem. Soc.* **1981**, *103*, 2667.

(33) Harris, W. R.; Raymond, K. N. *J. Am. Chem. Soc.* **1979**, *101*, 6534.

(34) Pecoraro, V.; Weilt, F. L.; Raymond, K. N. *J. Am. Chem. Soc.* **1981**, *103*, 5133.

(35) Stack, T. D. P.; Hou, Z.; Raymond, K. N. *J. Am. Chem. Soc.* **1993**, *115*, 6466.

(36) Tse, B.; Kishi, Y. *J. Am. Chem. Soc.* **1993**, *115*, 7892.

(37) Karpishin, T. K.; Dewey, T. M.; Raymond, K. N. *J. Am. Chem. Soc.* **1993**, *115*, 1842.

(38) Corey, E. J.; Bhattacharyya, S. *Tetrahedron Lett.* **1977**, *45*, 3919.

(39) Rastetter, W. H.; Erickson, T. J.; Venuti, M. C. *J. Org. Chem.* **1980**, *45*, 5011.

(40) Rastetter, W. H.; Erickson, T. J.; Venuti, M. C. *J. Org. Chem.* **1981**, *46*, 3579.

(41) Shanzer, A.; Libman, J.; Lifson, S.; Felder, C. E. *J. Am. Chem. Soc.* **1986**, *108*, 7609.

(42) Marínez, E. R.; Salmassian, E. K.; Lau, T. T.; Gutierrez, C. G. *J. Org. Chem.* **1996**, *61*, 3548. Ramírez, R. J. A.; Karamanukyan, L.; Ortiz, S.; Gutierrez, C. G. *Tetrahedron Lett.* **1997**, *38*, 749.

(43) Considine, W. J. *J. Organomet. Chem.* **1966**, *5*, 263.

8H). (+)-FABMS:  $m/z$  555 (MH<sup>+</sup>), isotope pattern consistent with formula. Anal. Calcd (Found) for C<sub>20</sub>H<sub>44</sub>O<sub>4</sub>Sn<sub>2</sub>: C, 41.0 (41.3); H, 7.57 (7.48).

**Methyl *N*-trityl-L-serinate (2).** To an ice cold slurry of methyl L-serinate hydrochloride in chloroform (25 g, 0.16 mol) was added 48.5 g (0.49 mol) triethylamine. Solid triphenylmethyl chloride (50 g, 0.18 mol) was added over 3 h. The solution was allowed to warm to room temperature and stirred overnight. The organic solution was washed with 5% citric acid (3 × 100 mL), water (3 × 100 mL), and brine (3 × 100 mL). The solution was dried over MgSO<sub>4</sub>, filtered, and evaporated to dryness. Recrystallization from benzene:hexanes gave a beige crystalline material. Yield: 77%. Mp: 146 °C (lit. mp 148 °C).<sup>44</sup> FT IR (thin film CHCl<sub>3</sub> cast):  $\nu$  1703 cm<sup>-1</sup>. Anal. Calcd (Found) for C<sub>23</sub>H<sub>23</sub>NO<sub>3</sub>: C, 80.90 (81.20); H, 6.79 (6.63); N, 12.31 (12.27).

**Tris(*N*-trityl-L-serine) Trilactone (3).** Methyl *N*-trityl-L-serinate (2) (50 g, 0.2 mol) and stannoxane (1) (12 g, 17.8 mmol) were added to a flask fitted with a condenser and a Dean–Stark trap filled with 4 Å molecular sieves. The reaction mixture was refluxed under a nitrogen atmosphere in toluene for 3 days. After cooling, the solution was evaporated to dryness to get a beige solid. The solid was dissolved in methylene chloride and purified on a flash silica plug. Evaporation of solvent gave the product as a white powder. Yield: 56%. FT IR (thin film CH<sub>2</sub>Cl<sub>2</sub> cast):  $\nu$  1735 cm<sup>-1</sup>. <sup>1</sup>H NMR (400 MHz, CDCl<sub>3</sub>):  $\delta$  2.65 (d,  $J$  = 6 Hz, 3H), 3.45 (m, 6H), 4.05 (t,  $J$  = 10.4 Hz, 3H), 7.2–7.5 (m, 27H). <sup>13</sup>C NMR (400 MHz, CDCl<sub>3</sub>):  $\delta$  54.7, 66.2, 71.1, 126.7, 128.0, 128.6, 145.5, 172.2. (+)-FABMS:  $m/z$  988 (M<sup>+</sup>), 744 (M<sup>+</sup> – trityl), 243 (trityl group). Anal. Calcd (Found) for C<sub>66</sub>H<sub>57</sub>N<sub>3</sub>O<sub>6</sub>: C, 80.22 (80.51); H, 5.81 (5.65); N, 4.25 (4.03). The preparation was repeated with 10 g of methyl *N*-trityl-L-serine to give 2.3 g of the enantioenterobactin precursor D-serinate trilactone.

**Triserine Trilactone Trihydrochloride (4).** To a slurry of 1 g of 3 in 25 mL degassed ethanol was added 1.5 mL of HCl (0.404 M) in dry, degassed ethanol, and the slurry was brought to reflux in a preheated oil bath for 15 mins. The reaction flask was cooled in an ice bath, and roughly half of the solvent was removed *in vacuo*, keeping the solvent cold. The solid material was quickly filtered, while kept under a gently blowing dry nitrogen stream, and washed with ethanol, chloroform, and ether. Yield: 98%. FT IR (KBr pellet):  $\nu$  1776 cm<sup>-1</sup>. <sup>1</sup>H NMR (500 MHz, DMSO-*d*<sub>6</sub>):  $\delta$  4.29 (dd,  $J$  = 12.5 Hz,  $J'$  = 2.46 Hz, 3H), 4.60 (s, 3H), 5.09 (dd,  $J$  = 12.5 Hz,  $J'$  = 1.69 Hz, 3H), 9.25 (br s, 9H). This material was not further characterized.

**3-(Benzyloxy)-1-methyl-2(1*H*)-4-carboxylpyridinone Chloride (5).** To a chilled slurry of 3-(benzyloxy)-1-methyl-2-oxo-1*H*-pyridine-4-carboxylic acid (2.0 g, 0.8 mmol) in freshly distilled benzene was added oxalyl chloride (1.0 g, 0.8 mmol). Addition of DMF (~0.1 mL) catalyzed the reaction. The solution was stirred for 1 h and evaporated to dryness at ~5 °C. The remaining yellow oil was dissolved in methylene chloride and used without further purification.

***N,N,N'*-Tris[(3-(benzyloxy)-1-methyl-2-oxo-1*H*-pyridin-4-yl)carbonyl]cyclotriseryl Trilactone, Benzyl-Protected Hopobactin (6).** 5 (10 equiv) was added quickly to a chilled solution of 4 (0.3 g) containing 10 equiv of triethylamine in methylene chloride (20 mL). After 1 h the solvent volume was reduced to ~1 mL. The remaining solution was applied to a silica gel column eluted with chloroform and 2% ethanol. The first several fractions were combined and washed with 5% citric acid, water, and brine. The organic solution was dried with MgSO<sub>4</sub> and filtered, and the volume was reduced. The remaining solution was applied to a rotary chromatograph and compound 6 was eluted using solvent gradient (3–0% hexanes in methylene chloride followed by 0–2% methanol). Yield: 3% (based on triamine). <sup>1</sup>H NMR (300 MHz, CDCl<sub>3</sub>):  $\delta$  3.56 (s, 9H), 4.07 (q,  $J$  = 11 Hz,  $J'$  = 7.1 Hz, 3H), 4.18 (q,  $J$  = 11 Hz,  $J'$  = 4.4 Hz, 3H), 4.8 (m,  $J$  = 7.1 Hz,  $J'$  = 4.4 Hz, 3H), 5.44 (d,  $J$  = 9.5 Hz, 3H), 5.51 (d,  $J$  = 9.5 Hz, 3H), 6.65 (d,  $J$  = 7.2 Hz, 3H), 7.1–7.4 (m, 18H), 8.55 (d,  $J$  = 7.1 Hz, 3H). (+)-FABMS:  $m/z$  985 (MH<sup>+</sup>), 894 (MH<sup>+</sup> – Bnz).

***N,N,N'*-Tris[(3-hydroxy-1-methyl-2-oxo-1*H*-pyridin-4-yl)carbonyl]cyclotriseryl Trilactone, Hopobactin (7).** Compound 6 (20 mg) was dissolved in a 1:1:1 mixture of ethanol:methanol:ethyl acetate (50 mL total). To this was added 10% Pd on carbon catalyst (<2 mg) and

two drops of acetic acid. The reaction mixture was stirred under H<sub>2</sub> gas for 10 min. The deprotected ligand precipitated as a yellow solid. Much of the ligand adhered to the carbon catalyst as a gel, so the catalyst was repeatedly washed with hot ethanol. Yield: 54%. <sup>1</sup>H NMR (300 MHz, DMSO-*d*<sub>6</sub>):  $\delta$  3.46 (s, 9H), 4.39 (dd,  $J$  = 11 Hz,  $J'$  = 4.4 Hz, 3H), 4.49 (dd,  $J$  = 11 Hz,  $J'$  = 7.4 Hz, 3H), 4.90 (m,  $J$  = 7.4 Hz,  $J'$  = 4.4 Hz, 3H), 6.48 (d,  $J$  = 7.2 Hz, 3H), 7.19 (d,  $J$  = 7.2 Hz, 3H), 8.81 (d,  $J$  = 7.02, 3H). <sup>1</sup>H NMR (300 MHz, CDCl<sub>3</sub>):  $\delta$  3.46 (s, 9H), 4.44 (dd,  $J$  = 11.6 Hz,  $J'$  = 1.8 Hz, 3H), 5.0 (dd,  $J$  = 11.6 Hz,  $J'$  = 3.4 Hz, 3H), 5.25 (br d,  $J$  = 7.9 Hz, 3H), 6.68 (s, 6H), 8.65, (d,  $J$  = 7.9 Hz, 3H). <sup>13</sup>C NMR (400 MHz, DMSO-*d*<sub>6</sub>):  $\delta$  37.2, 52.4, 65.7, 104.8, 116.8, 126.7, 146.8, 158.5, 166.9, 168.0. (+)-FABMS:  $m/z$  714 (MH<sup>+</sup>). HRMS Calcd (Found) for C<sub>30</sub>H<sub>31</sub>N<sub>6</sub>O<sub>15</sub>:  $m/z$  715.18680 (715.18474).

**Ferric Hopobactin (8).** Ferric acetylacetonate (1 equiv) in methanol was added to 1 equiv of 7 dissolved in methylene chloride. The solution immediately turned dark red and was allowed to stir for 2 h. The ferric complex was purified by flash chromatography on silica gel (methylene chloride:methanol 96:4 v/v). Crystals of the neutral complex were grown in a variety of solvents: diffusion of ether into acetone, THF, or methylene chloride gave fused plates. (+)-FABMS:  $m/z$  768 (MH<sup>+</sup>).

**X-ray Crystal Structure of Tris(*N*-trityl-L-serine) Trilactone (3).** Crystals of the *N*-trityl trilactone scaffold were obtained by slow evaporation of the compound from a solution of CH<sub>2</sub>Cl<sub>2</sub> and CH<sub>3</sub>OH over a period of 2 weeks. A crystal of approximate dimensions 0.3 × 0.2 × 0.1 mm was mounted on a glass fiber in a droplet of Paratone oil. All measurements were made on a Siemens SMART diffractometer with graphite-monochromated Mo K $\alpha$  radiation.<sup>45</sup> The data were collected at –138(1) °C using the  $\omega$  scan technique with a total frame collection time of 30 s. Data analysis was performed using Siemens XPREP program.<sup>46</sup> No decay or absorption corrections were applied.

The structure was initially solved using SIR92 using the program teXsan.<sup>47</sup> The absolute configuration was established by the method of Flack.<sup>48</sup> After all the atoms were located, the data set was refined using the SHELXTL (Version 5) software package.<sup>46</sup> The structure was refined on  $F^2$  in the orthorhombic space group  $P2_12_12_1$  (no. 19) using full-matrix least squares. All non-hydrogen atoms in the molecule were refined anisotropically. Hydrogen atoms were calculated and refined on their respective carbon atoms. The final cycle of refinement converged to  $R_1$  = 0.0549 and  $R_2$  = 0.0926 for 676 parameters and 7394 reflections.

**X-ray Crystal Structure of Ferric Hopobactin.** Dark red plates of ferric hopobactin were grown from diffusion of ether into wet DMF (~5% water). A crystal of approximate dimensions 0.2 × 0.1 × 0.01 mm was mounted on a glass fiber in a droplet of Paratone oil. All measurements were made on a Siemens SMART diffractometer with graphite monochromated Mo K $\alpha$  radiation.<sup>45</sup> The data were collected at –101(1) °C using the  $\omega$  scan technique with a frame width of 0.3° and a total frame collection time of 30 s. The intensity data were extracted from the frames using the program SAINT and integration box parameters of 1.0 (XY) × 0.5° (Z) to a maximum  $2q$  value of 46.5°. Data analysis was performed using the Siemens XPREP program.<sup>46</sup> No decay correction was applied. A semiempirical absorption correction based on  $\psi$  scans was applied to the data with minimum and maximum transmission factors of 1.00 and 0.827, respectively.

The structure was solved by direct methods (SHELXTL Version 5 software) and refined on  $F^2$  in the space group  $P2_1$  (no. 4) using full-matrix least squares.<sup>46</sup> Although there was some indication of C-centering from the data, this was determined to be pseudosymmetry and not crystallographically imposed. The iron atoms and selected oxygen atoms were refined anisotropically, while the remaining non-hydrogen atoms were refined isotropically. Hydrogen atoms were calculated and refined on their respective carbon atoms. The final cycle

(45) SMART, Area-Detector Software Package; Siemens Industrial Automation, Inc.: Madison, WI, 1993.

(46) SHELXTL, Crystal Structure Determination Package; Siemens Industrial Automation, Inc.: Madison, WI, 1994.

(47) teXsan, Crystal Structure Analysis Package; Molecular Structure Corporation, 1992.

(48) Flack, H. D. *Acta Crystallogr.* **1983**, A39, 876.

(49) SAINT, SAX Area-Detector Integration Program v. 4.024; Siemens Industrial Automation, Inc.: Madison, WI, 1994.

(44) Guttman, S. *Helv. Chim. Acta* **1962**, 45, 2622.

of refinement was based on 10510 reflections, 87 restraints, and 1036 variable parameters and converged to  $R_1 = 0.1165$  and  $R_2 = 0.2661$ .

**Solution Thermodynamics. General Methods.** All titrant solutions were prepared using distilled water that was further purified by passing through a Millipore Milli-Q reverse osmosis cartridge system (resistivity 18 MW cm). Titrants were degassed by boiling for 1 h while being purged by argon. Solutions were stored under an atmosphere of purified argon (Ridox Oxygen Scavenger (Fisher) and Ascarite II (A. H. Thomas) scrubbers) in order to prevent absorption of oxygen and carbon dioxide. Carbonate-free 0.1 M KOH was prepared from Baker Dilut-It concentrate and was standardized by titrating against potassium hydrogen phthalate using phenolphthalein as an indicator. Solutions of 0.1 M HCl were similarly prepared and were standardized by titrating against the KOH solution to phenolphthalein endpoint. The combined pH glass electrode (Orion semimicro) filled with 3 M KCl (Orion filling solution) was calibrated in hydrogen ion concentration units ( $\text{p[H]} = -\log [\text{H}^+]$ ) by titrating 2.000 mL standardized HCl diluted in 50 mL of 0.100 M KCl (Mallinckrodt, ACS grade) with 4.200 mL of standardized KOH. The Nernst parameters of the electrode and the  $\text{pK}_w$  value ( $13.78 \pm 0.05$ ) were refined using a nonlinear least-squares program.<sup>50</sup> All titrations were performed using a Dosimat 665 (Metrohm) piston buret and an Accumet 925 (Fisher) pH meter, both instruments being controlled by an IBM-PC computer.<sup>32,51</sup> Errors are reported in parentheses and correspond to the standard deviations. In all titrations the  $\text{p[H]}$  was kept below 8 to prevent the hydrolysis of the trilactone ring.

**<sup>1</sup>H NMR Titration.** Due to the low solubility of hopobactin in water, ~6 mg of ligand was dissolved in 0.5 mL DMF-*d*<sub>7</sub> (Aldrich, % D > 99.5) and the resulting solution diluted to 1 mL with D<sub>2</sub>O (Aldrich, % D > 99.9). The titration was performed directly in the NMR tube by adding small amounts of ~10% diluted NaOD (Aldrich, 40% wt, % D > 99) or ~10% diluted DCl (Aldrich, 20% wt, % D > 99.5) solutions in D<sub>2</sub>O with a Hamilton microsyringe. The solution was purged with nitrogen prior to the pH measurements. Apparent values were measured with a 3 mm Ag/AgCl combined microelectrode (Mettler-Toledo) filled with 3 M KCl and an Accumet 925 (Fisher) pH meter. The electrode was calibrated with three aqueous buffer solutions (Fisher) at pH = 4.00, 6.98, and 10.00. The measured pH values were corrected for the deuterium effect and the presence of ~50% DMF using the equation  $\text{pH}^* = \text{pH}_{\text{mes}} + 0.05$ .<sup>52</sup> The NMR spectra were recorded on a 500 MHz Bruker AM500 spectrometer and referenced to dioxane ( $\delta = 3.75$  ppm).

**Spectrophotometric Titrations.** The apparatus and methods for spectrophotometric titrations have been described in detail elsewhere.<sup>53</sup> The path length of the quartz cell (Hellma, Suprasil) was 10 cm. All solutions were maintained at constant ionic strength (0.100 M KCl), under argon atmosphere and at constant temperature ( $25.0 \pm 0.2$  °C) by using a jacketed titration vessel fitted to a Lauda K-2/R water bath. To 40 mL of 0.100 M KCl, 10 mL of a freshly prepared ligand solution (3 mM in DMF:water) was added. The effect of DMF was neglected, since the final concentration was less than 0.4%. After the  $\text{p[H]}$  was decreased to about 3 with 0.1 M HCl, the ligand was titrated with standardized base to about  $\text{p[H]}$  8.0. The thermodynamic reversibility was checked by cycling each of two independent titrations from low to high  $\text{p[H]}$  and back to low  $\text{p[H]}$ . The data (including absorbances at 150 different wavelengths ranging between 250 and 400 nm,  $\text{p[H]}$  values, and respective volumes of about 45 solutions per titration) were analyzed to determine the protonation constants using the factor analysis program FINDCOMP and the nonlinear least-squares refinement program REFSPEC.<sup>53</sup>

**Spectrophotometric Competition Titrations.** The formation constant of the ferric hopobactin complex was determined by competition against *trans*-1,2-diaminocyclohexane-*N,N,N',N'*-tetraacetic acid monohydrate (CDTA, Aldrich, ACS grade 99%). For each of four independent titrations, fresh ferric hopobactin was prepared and purified

as above and added as a stock solution. Between 8 and 12 solutions were prepared in 10 mL volumetric flasks, containing ferric hopobactin (~8 mM), CDTA (99.9 mM), and 0.05 M 3-(*N*-morpholino)propane-sulfonic acid (MOPS, Sigma, Cell Culture) as a buffer. The  $\text{p[H]}$  of the solutions was adjusted to 6.3–8.0 and the ionic strength to 0.1 by addition of 1.0 M KOH and 1.0 M KCl respectively. The solutions were allowed to stand in the dark at room temperature for 1 week to ensure thermodynamic equilibrium prior to recording the  $\text{p[H]}$  values and absorption spectra (HP 8452A diode array spectrophotometer, 1 cm Hellma quartz cell). Absorbances at 25 wavelengths (10 nm intervals between 400 and 640 nm inclusive) were used by the program REFSPEC to calculate the overall formation constant.<sup>53</sup> Protonation constants of CDTA and the stability constant of FeCDTA used in the refinement were taken from the literature.<sup>54</sup>

**Electrochemical Measurements.** Cyclic voltammograms of a 0.35 mM ferric hopobactin solution in acetonitrile (Fisher) containing 0.1 M tetrabutylammonium perchlorate (Fluka, Electrochemical grade) as supporting electrolyte were recorded on a BAS100A electrochemical analyzer. Working and auxiliary platinum electrodes were used with a freshly prepared Pleskow reference electrode (0.01 M AgNO<sub>3</sub> in 0.1 M (C<sub>4</sub>H<sub>9</sub>)<sub>4</sub>NClO<sub>4</sub> in CH<sub>3</sub>CN/Ag). The half-wave potentials were also measured against the ferrocinium/ferrocene internal reference electrode.

## Results and Discussion

**Synthesis.** Previous methods of synthesizing the enterobactin scaffold were laborious and gave very low yields. Corey<sup>38</sup> and Rastetter<sup>39,40</sup> each obtained the scaffold in roughly 1% yield. Shanzer improved the synthesis with the use of a tin template, but the overall yield was still low (~6%) due to the low-yield formation of a serine  $\beta$ -lactone precursor.<sup>41</sup> Gutierrez et al. further developed the methodology used by Shanzer and obtained the trityl-protected trilactone in 54% yield.<sup>42</sup> Following these precedents and Seebach's syntheses of cyclopolyhydroxybutanoate derivatives,<sup>55,56</sup> a one-step synthesis of the protected enterobactin scaffold that eliminates the  $\beta$ -lactone intermediate was devised, as shown in Scheme 1.

Removal of the *N*-trityl protecting groups under acidic conditions gave the enterobactin scaffold triamine trihydrochloride (Scheme 2). Bidentate 3-hydroxy-1-methyl-2(1*H*)-pyridinonate groups (3,2-HOPO) were coupled via their acid chloride to the triamine scaffold. The 3,2-HOPO ligands were chosen because they have been identified in natural siderophores,<sup>57</sup> are easily activated for amide formation, and can be deprotected by reductive hydrogenation,<sup>58,59</sup> conditions in which the enterobactin scaffold is stable (Scheme 2). Hopobactin, like the other 3,2-HOPO derivatives, has low  $\text{pK}_a$ 's and a high affinity for iron(III) (*vide infra*). The ferric complex was obtained by combining at room temperature free ligand dissolved in methylene chloride with ferric acetylacetonate dissolved in methanol, followed by column chromatography purification. The complex could be further purified by recrystallization from DMF:ether. The one metal/one ligand stoichiometry was confirmed by mass spectroscopy.

**X-ray Crystal Structure of Tris(*N*-trityl-*L*-serine) trilactone (3).** The *N*-trityl trilactone is soluble in methylene chloride, chloroform, and hot toluene. Slow evaporation from a methylene chloride:methanol solution produced colorless crystals,

(54) Martell, A. E.; Smith, R. M. *Critical Stability Constants*; Plenum Press: New York, 1974–1981; Vols. 1–5.

(55) Plattner, D. A.; Brunner, A.; Dobler, M.; Müller, H.-M.; Petter, W.; Zbinden, P.; Seebach, D. *Helv. Chim. Acta* **1993**, *76*, 2004.

(56) Müller, H.-M.; Seebach, D. *Angew. Chem., Int. Ed. Engl.* **1993**, *32*, 477.

(57) Meyer, J.-M.; Hohnadel, D.; Hallé, F. J. *Gen. Microbiol.* **1989**, *135*, 1479.

(58) Xu, J.; Kullgren, B.; Durbin, P. W.; Raymond, K. N. *J. Med. Chem.* **1995**, *38*, 2606.

(59) Xu, J.; Franklin, S. J.; Whisenhunt, D. W.; Raymond, K. N. *J. Am. Chem. Soc.* **1995**, *117*, 7245.

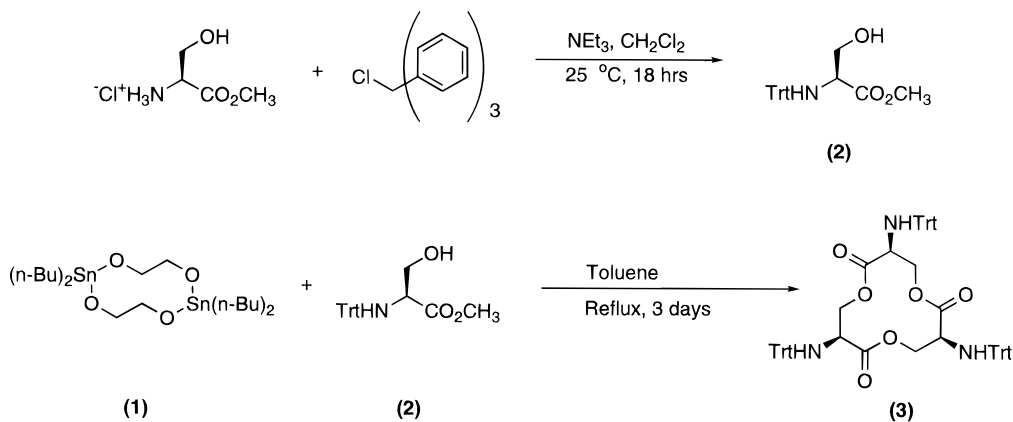
(50) Martell, A. E.; Motekaitis, R. M. *The Determination and Use of Stability Constants*; VCH: New York, 1988.

(51) Kappel, M.; Raymond, K. N. *Inorg. Chem.* **1982**, *21*, 3437.

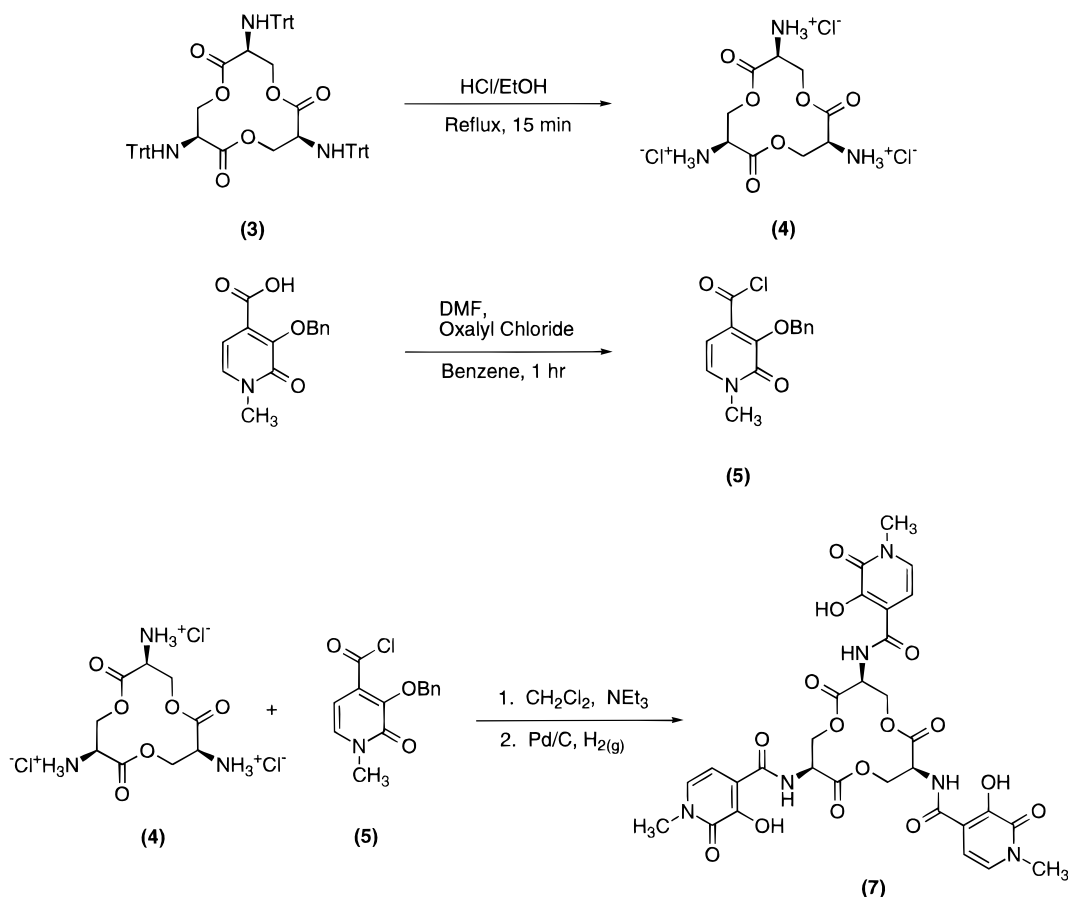
(52) Perrin, D. D.; Dempsey, B. *Buffers for pH and Metal Ion Control*; Chapman and Hall: London, 1974.

(53) Turowski, P. N.; Rodgers, S. J.; Scarrow, R. C.; Raymond, K. N. *Inorg. Chem.* **1988**, *27*, 474.

## Scheme 1



## Scheme 2



with a needlelike morphology. An X-ray analysis conforms to an earlier report<sup>41</sup> that included a cogent discussion of the stereochemistry, but no full report of the structure. To provide atom coordinates and a comparison structure, a full analysis was performed.

The *N*-trityl trilactone displays an unusual geometry for cyclic trilactone compounds (Figure 2). Of those enterobactin analogs that have been structurally characterized, all that have homochiral stereocenters, including ferric hopobactin (*vide infra*), adopt a geometry with the carbonyl moieties in a *cis* conformation.<sup>37,60,61</sup> These groups in the *N*-trityl structure adopt a *trans* conformation with two carbonyl groups on one face of the

macrocyclic ring and one other on the opposite face. A *trans* conformation has been observed in other examples only when the stereocenters are heterochiral.<sup>55</sup> Of the three *N*-trityl amine substituents, two occupy equatorial sites, while the third occupies an axial site on the macrocycle.

Superpositions of the trilactone rings from the *N*-trityl scaffold and [V(enterobactin)]<sup>2-</sup> display significantly dissimilar conformations, as shown in Figure 2. A least-squares fitting of the 12 atoms that comprise the macrocycles give a root mean squares (RMS) deviation of 0.6 Å. The general form of the macrocyclic rings are the same.<sup>28,61</sup> However, the amide nitrogens and serine carbonyl oxygens adopt the *all-cis* conformation in [V(enterobactin)]<sup>2-</sup> requisite for metal coordination, which overlap poorly with the *trans* conformation in the trityl-protected macrocycle.<sup>28</sup> A comparison of the *N*-trityl trilactone and the ferric hopobactin macrocycle (*vide infra*) leads to the

(60) Shanzer, A.; Libman, J.; Frolow, F. *J. Am. Chem. Soc.* **1981**, *103*, 7339.

(61) Seebach, D.; Muller, H.-M.; Burger, H. M.; Plattner, D. A. *Angew. Chem., Int. Ed. Engl.* **1992**, *31*, 434.

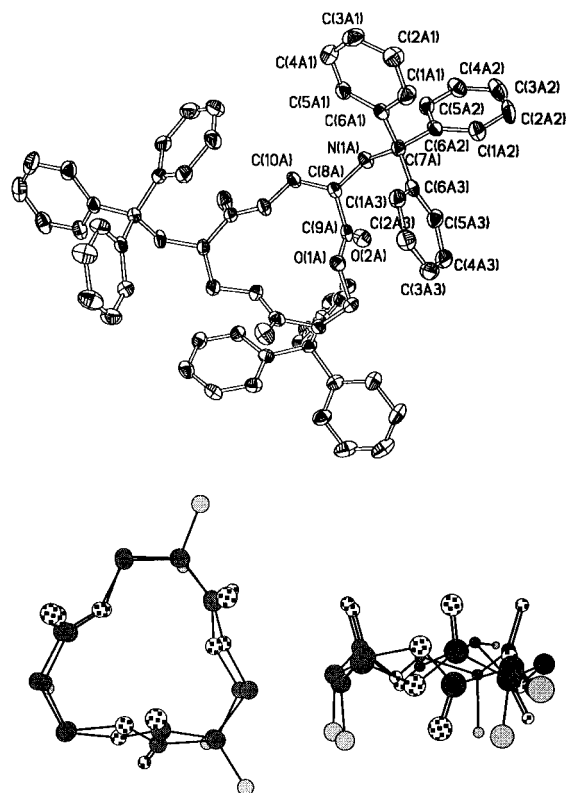


**Figure 2.** An ORTEP diagram (top) of the tris(*N*-trityl-L-serine) trilactone (**3**) (hydrogen atoms are omitted for clarity). The numbering scheme is indicated for one third of the molecule only. A CHEM3D overlay (bottom) of the triserine trilactone from **3** and V(enterobactin)<sup>2-</sup> viewed down (left) and perpendicular to (right) the approximate molecular 3-fold axis. The RMS error in atom positions is 0.600 Å.

same conclusion: the trityl protecting groups are too bulky to conform to the *all-cis* conformation. The structure of the *N*-trityl trilactone essentially establishes a limit on the predisposition for complex formation of derivatives of the macrocycle.

**X-ray Crystal Structure of Ferric Hopobactin.** The ferric hopobactin complex crystallizes in the monoclinic space group  $P2_1$  with  $Z = 8$  (Table 1). The absolute configuration was established by the method of Flack.<sup>48</sup> The very small crystal (0.01 mm in one dimension) gave a low intensity data set with many weak reflections, especially at high scattering angles, and resulted in a low-resolution structure. However, the quality of the analysis is more than adequate for establishing the coordination and molecular geometry (Figure 3). The generally low intensities of reflections where  $h + k$  values are odd suggested that the cell might be C centered. However, a significant number of apparent violations ( $I/\sigma(I) > 30$ ) and the final structure showed that this is pseudo C centering of the iron atoms, with significant deviations in the remaining parts of the apparently C-centered related molecules.

The complex shown in Figure 3 is a trischelate with approximate  $C_3$  point symmetry. Since the trilactone scaffold is based on three L-serine units, the introduction of chirality at the metal center produces a preferred diastereoisomeric neutral complex. The metal center has a right-handed configuration ( $\Delta$  chirality) as found for the vanadium(IV) structure.<sup>28</sup> The same configuration has also been determined by circular dichroism (CD) spectroscopy for the iron(III), chromium(III), and rhodium(III) enterobactin complexes.<sup>23,62</sup>

The average Fe–O distance for the 2-hydroxy oxygen is shorter by 0.08 Å than for the 3-carbonyl oxygen, typical of a

**Table 1.** Crystal Data and Structure Refinement for **3** and Ferric Hopobactin (**8**)

formula	$C_{66}H_{57}N_3O_6$	$FeC_{30}H_{28}N_6O_{15}$
formula weight	988.15	768.43
$T$ , °C	−138(1)	−101(1)
crystal system	orthorhombic	monoclinic
space group	$P2_12_12_1$ (no. 19)	$P2_1$ (no. 4)
$a$ , Å	9.2495(2)	13.0366(9)
$b$ , Å	11.3584(1)	22.632(2)
$c$ , Å	4.945(1)	27.130(2)
$\beta$		100.926°
$V$ , Å <sup>3</sup>	5142.1(2)	7859(1)
$Z$	4	8
$D_{\text{calcd}}$ , g cm <sup>−3</sup>	1.276	1.311
$\mu$ (Mo K $\alpha$ ), mm <sup>−1</sup>	0.082	0.455
$\theta$ range, deg	0.83 to 23.28	1.53 to 23.27
reflections collected	22178	31676
index ranges	−10 ≤ $h$ ≤ 6 −10 ≤ $k$ ≤ 12 −47 ≤ $l$ ≤ 54	−14 ≤ $h$ ≤ 13 −25 ≤ $k$ ≤ 23 −30 ≤ $l$ ≤ 23
independent reflections	7395 [ $R(\text{int}) = 0.0396$ ]	21051 [ $R(\text{int}) = 0.0981$ ]
data/restraints/parameter	7394/0/676	10510/87/1036
final $R$ indices ( $I > 2\sigma(I)$ ) <sup>a</sup>	$R_1 = 0.0448$ , $R_2 = 0.0926$	$R_1 = 0.1165$ , $R_2 = 0.2661$
goodness of fit <sup>b</sup>	1.117	1.171
largest diff. peak and hole	0.331 and −0.311 eÅ <sup>−3</sup>	1.038 and −0.428 eÅ <sup>−3</sup>

<sup>a</sup>  $R_1 = \sum(|F_o| - |F_c|)/\sum|F_o|$ ,  $R_2 = \{\sum[w(F_o^2 - F_c^2)^2]/\sum[wF_o^4]\}^{1/2}$ .  
<sup>b</sup> GOF =  $[\sum w(|F_o| - |F_c|)^2/(N_o - N_v)]^{1/2}$ , where  $w = 1/(\sigma^2|F_o|)$ .

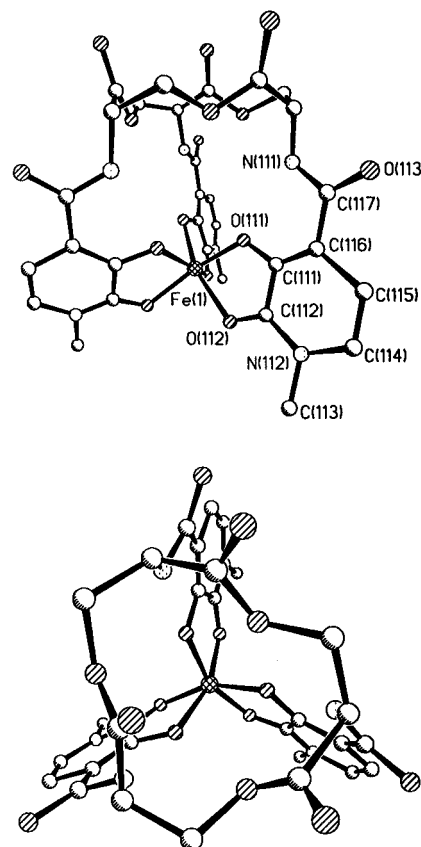


**Figure 3.** A view of one of two crystallographically independent ferric hopobactin complexes viewed (top) perpendicular to and (bottom) down the approximate molecular 3-fold axis (hydrogen atoms are omitted for clarity).

hydroxypyridinonate complex.<sup>63</sup> Average lengths over the four molecules in the asymmetric unit cell are 1.98(2) and 2.06(3) Å respectively. The 3,2-HOPO chelates twist from octahedral geometry (a 60° angle is expected for a perfect octahedron) around the coordination polyhedron of the central iron atom.

(62) Stack, T. D. P.; Karpishin, T. B.; Raymond, K. N. *J. Am. Chem. Soc.* **1992**, *114*, 1512.

The average twist angle, defined as the angle between two coordinating atoms projected onto the plane perpendicular to the idealized 3-fold axis, is  $35(2)^\circ$ . By comparison, the twist angle in vanadium(IV) enterobactin is only  $28^\circ$ .<sup>37</sup> Considering that the twist angles in iron(III) triscatecholate complexes are  $4\text{--}6^\circ$  larger than in the corresponding vanadium(IV) complexes,<sup>62,64–66</sup> the twist angle of iron(III) enterobactin has been estimated to be close to  $33^\circ$ ,<sup>37</sup> which is in excellent agreement with the value found for ferric hopobactin. The optimum twist angle in a trischelate metal complex has been predicted from the normalized bite of the bidentate chelating units (the normalized bite value is the distance between the two coordinating atoms of a chelate, divided by the metal–heteroatom bond length).<sup>67</sup> Since hydroxypyridinonates have two significantly different metal–oxygen distances, only an approximate normalized bite can be calculated. For ferric hopobactin the normalized bite value is 1.27 and the corresponding optimum twist angle based on the lowest repulsive energy between the ligating atoms is  $45^\circ$ .<sup>67</sup> This value is supported by the structure of the simple  $\text{Fe}(3,2\text{-HOPO})_3$  complex, which has a twist angle of  $42.1^\circ$ .<sup>63</sup> The substantially smaller twist angle observed in ferric hopobactin seems to be a result of steric constraints imposed by the rigid scaffold. For comparison, the complexes  $\text{V}(\text{TRENCAM})^{3-}$ ,<sup>68</sup>  $\text{Fe}(\text{TRENCAM})^{3-}$ ,<sup>62</sup>  $\text{V}(\text{Et}_3\text{MECAM})^{2-}$  [ $\text{Et}_3\text{MECAM} = 1,3,5\text{-tris}(\text{dihydroxybenzamidomethyl})\text{-}2,4,6\text{-triethylbenzene}$ ],<sup>69</sup> and  $\text{V}(\text{enterobactin})^{2-}$ <sup>37</sup> have twist angles  $4.8^\circ$ ,  $3.2^\circ$ ,  $6.6^\circ$ , and  $8.3^\circ$  smaller than their nontethered analogs  $\text{V}(\text{cat})_3^{3-}$  (cat = catechol),<sup>65</sup>  $\text{Fe}(\text{cat})_3^{3-}$ ,<sup>64</sup> and  $\text{V}(\text{eba})_3^{2-}$  (eba = *N*-ethyl-2,3-dihydroxybenzamide)<sup>37</sup> respectively.

Superposition of two molecules from the asymmetric unit shows some conformational differences, with a RMS deviation of atoms of  $0.461 \text{ \AA}$ . As seen in Figure 4, the predominant deviations occur in the tilting of the scaffold carbonyl groups relative to the plane of the macrocycle. The overlay of ferric hopobactin and  $\text{V}(\text{enterobactin})^{2-}$  molecules produces a RMS deviation of  $0.351 \text{ \AA}$ , showing that the structures are essentially identical. Thus, the rigid structure of vanadium(IV) enterobactin is not markedly perturbed by substituting the catecholamide by hydroxypyridinonate binding groups, nor by the somewhat smaller vanadium(IV) cation ( $r_1 = 0.58 \text{ \AA}$  for V(IV) and  $0.65 \text{ \AA}$  for Fe(III), respectively).<sup>70</sup>

**Spectroscopic Properties of Ferric Hopobactin.** The visible absorption spectrum of ferric hopobactin (Figure 6) shows two LMCT transitions centered at  $432 \text{ nm}$  ( $\epsilon = 6200 \text{ M}^{-1} \text{ cm}^{-1}$ ) and  $534 \text{ nm}$  ( $\epsilon = 5200 \text{ M}^{-1} \text{ cm}^{-1}$ ). The energy and intensity of the bands are typical for pseudooctahedral ferric trishydroxypyridinonate complexes. The chirality of the ferric hopobactin complex was probed by circular dichroism spectroscopy. Figure 7 shows the CD spectrum recorded in pure methanol. The band at  $340 \text{ nm}$  is due to the chiral trilactone scaffold. Two additional transitions are observed in the visible region at  $410 \text{ nm}$  and  $550 \text{ nm}$ . These bands arise from ligand-

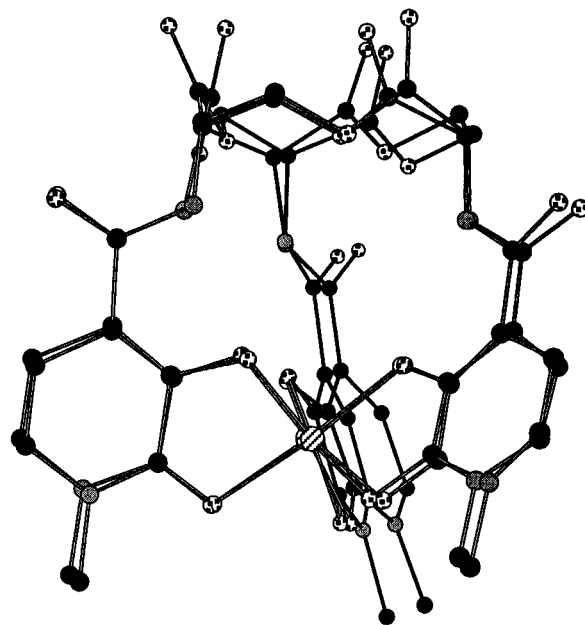


**Figure 4.** A CHEM3D overlay of two conformationally different ferric hopobactin molecules from the asymmetric unit (hydrogen atoms are omitted for clarity). The RMS error in atom positions is  $0.461 \text{ \AA}$ .

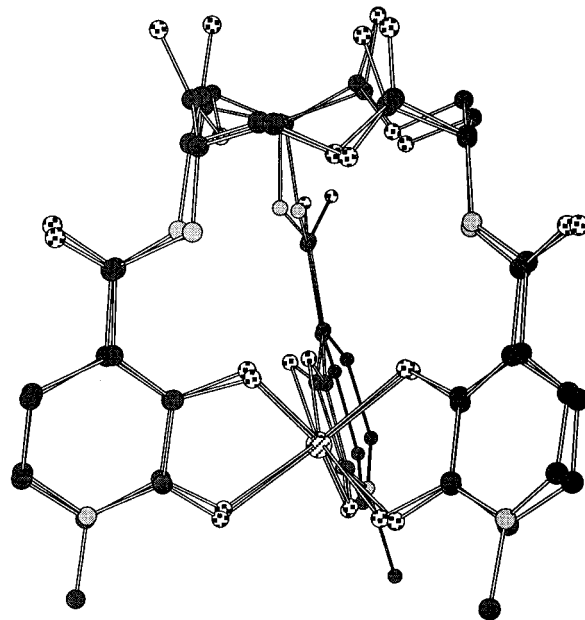


**Figure 5.** A CHEM3D overlay of ferric hopobactin and  $\text{V}(\text{enterobactin})^{2-}$  based on the atomic coordinates from the X-ray structures (hydrogen atoms are omitted for clarity). The RMS error in atom positions is  $0.351 \text{ \AA}$ .

to-metal charge transfer (LMCT) transitions and are therefore sensitive to the chirality at the metal center.<sup>71</sup> The CD spectrum of ferric enterobactin (Figure 7) also shows two LMCT bands of the same sign and magnitude as the transitions of ferric hopobactin. On the basis of these similarities, the ferric hopobactin spectrum is fully consistent with the assigned D absolute configuration and represents the first chiral hydroxypyridinonate complex.

**Ligand Protonation Constants.** The hopobactin ligand is a triprotic acid. Its low solubility in water prevents the determination of the stepwise protonation constants by potentiometry. Therefore, a  $^1\text{H}$  NMR potentiometric titration was

(63) Scarrow, R. C.; Riley, P. E.; Abu-Dari, K.; White, D. L.; Raymond, K. N. *Inorg. Chem.* **1985**, *24*, 954.

(64) Raymond, K. N.; Isied, S. S.; Brown, L. D.; Fronczek, F. R.; Nibert, J. H. *J. Am. Chem. Soc.* **1976**, *98*, 1767.

(65) Cooper, S. R.; Koh, Y. B.; Raymond, K. N. *J. Am. Chem. Soc.* **1982**, *104*, 5092.

(66) Karpishin, T. B.; Stack, T. D. P.; Raymond, K. N. *J. Am. Chem. Soc.* **1993**, *115*, 182.

(67) Kepert, D. L. *Inorganic Stereochemistry*; Springer-Verlag: Berlin, 1982.

(68) Bulls, A. R.; Pippin, C. G.; Hahn, F. E.; Raymond, K. N. *J. Am. Chem. Soc.* **1990**, *112*, 2627.

(69) Hou, Z.; Stack, T. D. P.; Sunderland, C. J.; Raymond, K. N. *Inorg. Chim. Acta* **1997**, submitted for publication.

(70) Shannon, R. D. *Acta Crystallogr.* **1976**, *A32*, 751.

(71) Karpishin, T. B.; Gebhard, M. S.; Solomon, E. I.; Raymond, K. N. *J. Am. Chem. Soc.* **1991**, *113*, 2977.

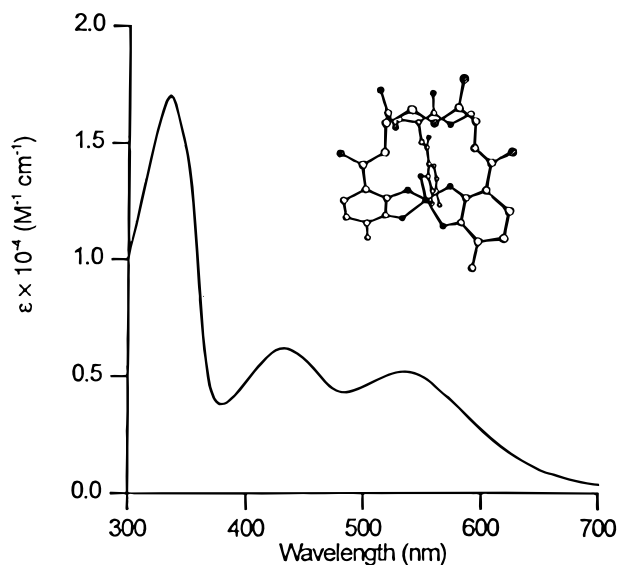


**Figure 6.** The UV-vis absorption spectrum of ferric hopobactin in pure methanol.  $T = 22\text{ }^{\circ}\text{C}$ .

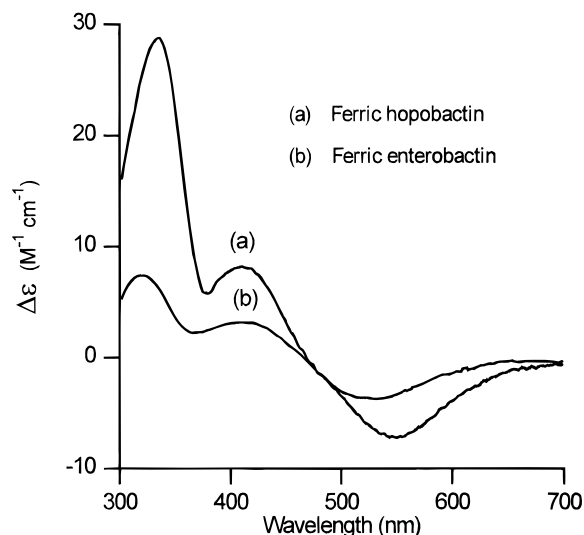


**Figure 7.** Circular dichroism spectra of (a) ferric hopobactin in pure methanol and (b) ferric enterobactin in water.  $T = 22\text{ }^{\circ}\text{C}$ .

carried out in a mixed DMF- $d_7$ :D $_2$ O (~1:1 v/v) solvent system. The two aryl protons of the three equivalent 3,2-HOPO groups, which appear as an AB system, were suitable nuclei to observe the protonation of the free ligand. The assignment and chemical shift changes for the aryl region of the  $^1\text{H}$  NMR spectra as a function of  $\text{pH}^*$  are depicted in Figure 8. Over the  $\text{pH}^*$  range 2–8, the higher field signal (assigned to proton  $\text{H}_b$  in the para position with respect to the hydroxyl protonation site) showed no significant shift. In contrast, the lower field signal (assigned to proton  $\text{H}_a$  located in the meta position) shifts from  $\delta = 7.17$  to 6.59 ppm, as  $\text{pH}^*$  increases from 5 to 8, with only one inflection point at  $\text{pH}^* = 6.0(2)$ . Although full deprotonation is not achieved at  $\text{pH}^* = 8$ , the basicity was not further increased in order to prevent hydrolysis of the trilactone scaffold.

The protonation properties of the chelator were further investigated by UV absorption spectroscopy up to  $\text{p}[\text{H}]$  8 as shown in Figure 9. Below  $\text{p}[\text{H}]$  3 the fully protonated ligand shows a broad absorption band at 330 nm assigned to a hydroxypyridinone-centered  $\pi \rightarrow \pi^*$  transition. As the  $\text{p}[\text{H}]$  is raised, this band undergoes a progressive bathochromic and hyperchromic shift. Simultaneously, an additional broad, unresolved band appears at approximately 340 nm. This

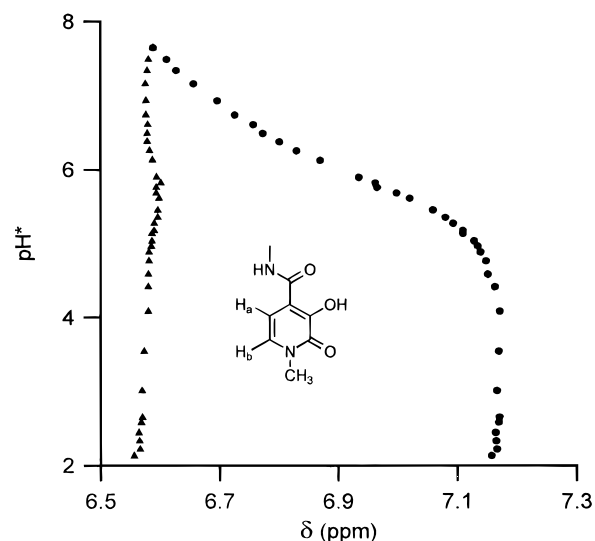


**Figure 8.** Variations of the  $^1\text{H}$  NMR chemical shifts recorded at 500 MHz for the aryl protons of hopobactin ( $\text{H}_a$  (●) and  $\text{H}_b$  (▲)) as a function of  $\text{pH}^*$  in DMF- $d_7$ :D $_2$ O 50:50 v/v.  $T = 22\text{ }^{\circ}\text{C}$ ; and  $[\text{hopobactin}] \sim 8\text{ mM}$ .

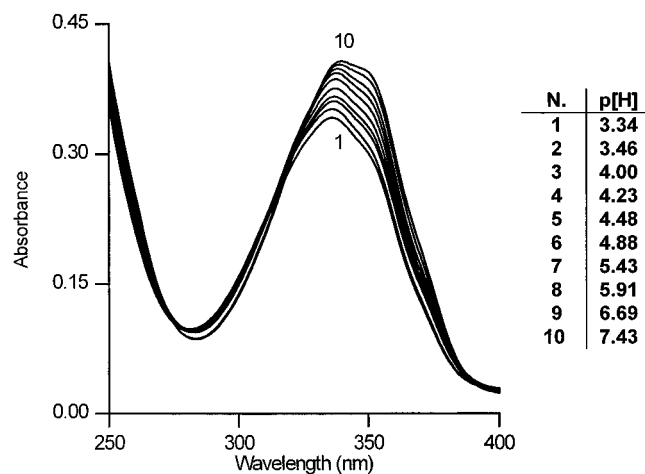


**Figure 9.** Spectrophotometric titration of hopobactin by KOH.  $I = 0.1\text{ KCl}$ ;  $T = 25.0(2)\text{ }^{\circ}\text{C}$ ;  $l = 10\text{ cm}$ ;  $[\text{hopobactin}] = 0.6\text{ mM}$ ; and  $[\text{KOH}] = 0.1\text{ M}$ .

behavior is consistent with a deprotonation of the chelating units.

Factor analysis of the spectrophotometric data recorded between 250 and 400 nm indicated the presence of only two distinct absorbing species in solution. Therefore, analysis of the data with a model involving four independent absorbing species (deprotonated, monoprotated, diprotated, and triprotated) was not successful in giving values for the protonation constants  $K_{011}$ ,  $K_{012}$ , and  $K_{013}$  defined by

$$\text{LH}_{n-1}^{n-4} + \text{H}^+ \rightleftharpoons \text{LH}_n^{n-3}$$

$$K_{01n} = \frac{[\text{LH}_n^{n-3}]}{[\text{LH}_{n-1}^{n-4}][\text{H}^+]} \quad (1)$$

$$\beta_{013} = K_{011}K_{012}K_{013}$$

The data were refined successfully using a model including only protonated ( $\text{LH}_3$ ) and deprotonated ( $\text{L}^{3-}$ ) ligand. This suggests that the spectroscopic properties of the mono- and diprotated species are linear combinations of the spectra of the fully protonated and deprotonated ligand. Refinement of the overall



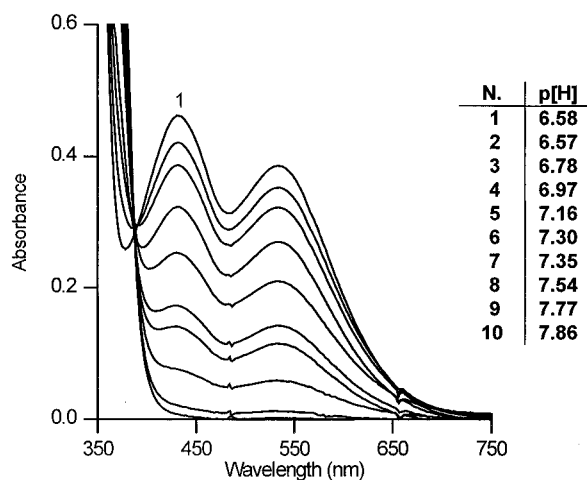
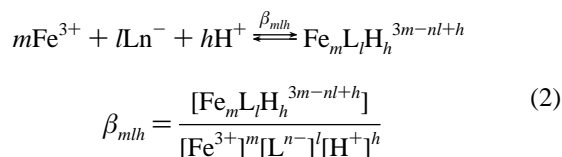


**Figure 10.** Spectrophotometric competition titration of ferric hopobactin by KOH in the presence of CDTA. [MOPS] = 0.05 M;  $I = 0.1$  KCl;  $T = 22(2)^\circ\text{C}$ ;  $l = 10$  cm; [Fehopobactin] = 7.8 mM; and [CDTA] = 99.9 mM. Spectrum 1 corresponds to the pure complex.

protonation constant yielded a  $\log \beta_{013}$  of 18.2(3), which gives an average protonation constant  $\log K_{av}$  of 6.1 to each proton. This value agrees well with the value estimated from the NMR titration, those of TRENHOPO ( $\log K_{av} = 5.9$ , disregarding the central amine proton),<sup>72</sup> and those of the monochelate model compound 1-methyl-4-(*n*-propylamido)-3,2-hydroxypyridinone ( $\log K_{011} = 6.12$ ).<sup>58</sup> This behavior can be predicted, because the hydroxypyridinonate units are identical and well isolated. If the microscopic protonation constants are identical, the macroscopic constants for the three steps would be equal to  $K_{av}/3$ ,  $K_{av}$ , and  $3K_{av}$ .<sup>73</sup> However, the ratio of two successive protonation constants for the hexadentate catecholamides and TRENHOPO is at least twice the value calculated for a statistical distribution.<sup>31,32,59</sup> A comparable behavior is expected in the case of hopobactin. Indeed, the large absorbance increase between p[H] 3.3 and 4.5 indicates a greater than statistical separation of the protonation constants around the average value.

**Stability of Ferric Hopobactin.** The metal vs proton affinity of hopobactin is sufficiently large that the stability constant cannot be determined directly. In an attempt to investigate the protonation behavior of the ferric hopobactin complex, spectrophotometric titrations were performed. The iron complex is stable in acidic conditions and shows no evidence of protonation at low p[H]: no changes in the absorption spectrum could be observed down to p[H] 2, suggesting that the complex remains intact. Even the addition of 1.0 M HCl to dilute solutions of ferric hopobactin induced no spectroscopic change after 12 h. Therefore, the formation constant  $\beta_{110}$  (eq 2) was determined by spectrophotometric competition experiments.



The stability constant of the ferric hopobactin was measured by competition against 10-fold excess of CDTA over the p[H] range 6.3–8.0 (Figure 10). Under these conditions, almost no exchange can be seen at p[H] 6.3, whereas complete exchange is observed around p[H] 7.5. At this p[H] the hydrolysis of the enterobactin trilactone scaffold is negligible. Due to slow exchange rates, the competition titrations were performed over

1 week. The rigidity of the competitor, the steric hindrance of the ferric hopobactin complex, and the high p[H] values, account for the slow kinetics encountered to reach equilibrium.<sup>74</sup> The existence of an isosbestic point at 388 nm suggests that no ternary iron–CDTA–hopobactin species forms in a significant concentration.

The actual competition equilibrium can be expressed by the following equations:



$$K_{\text{comp}} = \frac{[\text{FeCDTA}]_{\text{tot}}[\text{L}]_{\text{tot}}}{[\text{FeL}][\text{CDTA}]_{\text{tot}}} = \frac{\beta'_{110} \alpha^{\text{FeCDTA}} \alpha^{\text{L}}}{\beta_{110} \alpha^{\text{CDTA}}} \quad (4)$$

where L, CDTA, and FeCDTA refer to all forms of unbound hopobactin, CDTA, and iron(III)-complexed CDTA respectively.

$$[\text{L}]_{\text{tot}} = [\text{L}^{3-}] + [\text{LH}^{2-}] + \dots + [\text{LH}_3]$$

$$[\text{CDTA}]_{\text{tot}} = [\text{CDTA}^{4-}] + [\text{CDTAH}^{3-}] + \dots + [\text{CDTAH}_4]$$

$$[\text{FeCDTA}]_{\text{tot}} = [\text{FeCDTA}^-] + [\text{FeCDTA}(\text{OH})^{2-}]$$

The  $a^{\text{L}}$ ,  $a^{\text{CDTA}}$ , and  $a^{\text{FeCDTA}}$  coefficients are defined elsewhere.<sup>75</sup> With the known protonation constants of hopobactin and CDTA ( $\log K_{011} = 12.4$ ,  $\log K_{012} = 6.15$ ,  $\log K_{013} = 3.53$ ,  $\log K_{014} = 2.42$ ),<sup>54</sup> the complexation ( $\log \beta'_{110} = 30$ )<sup>54</sup> and hydroxylation ( $\log \beta'_{111} = 20.30$ )<sup>54</sup> constants of ferric CDTA,  $\beta_{110}$  was refined using a nonlinear least-squares method.<sup>53</sup> The average formation constant of ferric hopobactin, from three independent titrations, was determined to be  $\log \beta_{110} = 26.4$ –(3).

Hopobactin provides for the first time the opportunity to directly assess the contribution toward metal binding of the predisposition induced by the macrocyclic triserine scaffold on chelating groups other than catecholamides. The almost identical formation constant of ferric hopobactin and ferric TRENHOPO clearly indicates that the trilactone scaffold does not induce additional stabilization for hydroxypyridinonate ligands. In contrast, ferric enterobactin is more stable than model compounds, such as TRENAM or MECAM (1,3,5-tris-(dihydroxybenzamidomethyl)benzene), by a factor of  $10^6$ .<sup>19,31</sup> Although the structures of the hopobactin and enterobactin free ligands are not known, the structural comparison of the vanadium(IV) enterobactin scaffold with related trilactones synthesized by Shanzer et al.,<sup>60</sup> or the cyclic trilactones of polyhydroxybutyric acids prepared by Seebach et al.,<sup>61</sup> suggests that there is very little reorganization of the ligand upon complexation. Indeed, a least-squares analysis of the overlay of the vanadium(IV) enterobactin scaffold<sup>28</sup> and Seebach's trilactone<sup>55</sup> gives a root mean-squares deviation of atom positions of only 0.069 Å, whereas a significantly higher RMS deviation (0.309 Å) is found with the ferric hopobactin scaffold (Figure 11). Empirical force field calculations<sup>41</sup> and analysis of the X-ray structures of the free Et<sub>3</sub>MECAM ligand and its vanadium(IV) complex<sup>35</sup> provide additional evidence that the ground state of the enterobactin scaffold is the same in the free and metal-complexed form. These structures show that the only degree of freedom is in the rotation of each of the catechol groups. The predisposition of the pendant catecholamide

(74) Albrecht-Gary, A. M.; Palanche-Passeron, T.; Rochel, N.; Hennard, C.; Abdallah, M. A. *New J. Chem.* **1995**, *19*, 105.

(75) Ringbom, A. *Complexation in Analytical Chemistry*; Interscience: New York, 1963.

(72) Xu, J.; Raymond, K. N. Unpublished results.

(73) Perlmutter-Hayman, B. *Acc. Chem. Res.* **1986**, *19*, 90.

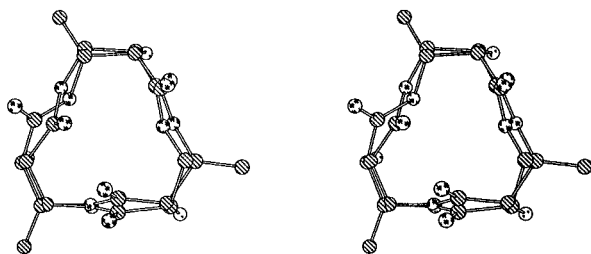


**Figure 11.** A Stereoview overlay of the crystallographic structures of the ferric hopobactin scaffold with Seebach's trilactone (ref 61). The RMS error in atom positions is 0.309 Å.

binding units which are oriented to one face of the scaffold in Et<sub>3</sub>MECAM, or in the analog synthesized by Tse and Kishi (based on three fused cyclohexyl rings in chair conformation), reduces the conformational space the chelates can occupy.<sup>35,36</sup> This induces an increase in the overall stability of the complex. For example, Et<sub>3</sub>MECAM gains 10<sup>3</sup> in stability over MECAM, and the saturated analog of Tse and Kishi has a stability constant with ferric ion that is the same as enterobactin.<sup>36</sup> The free energy advantage<sup>26</sup> of enterobactin over its analogs is derived from the scaffold architecture.

The variation of the stability constants on going from bidentate to hexadentate catecholamide, hydroxamate, and 3,2-hydroxypyridinonate ligands based on the TREN and enterobactin scaffolds are given in Table 2. Although no data are yet available for a hydroxamic acid analog of enterobactin, the magnitude of the formation constant for an iron(III) hydroxamate complex is the same whether the binding groups are part of a hexadentate molecule or three independent bidentate ligands. Initially pointed out by Schwarzenbach and Schwarzenbach,<sup>76</sup> and later emphasized by Carrano et al.,<sup>77</sup> the free energy per hydroxamate group is constant at a standard state of 1 M. Interestingly, this apparent lack of chelate effect seen for the hydroxamate-based ligands is more general and can be extended to the more basic catecholamide chelators such as TRENCAM (Table 2) or MECAM. As discussed above, the large "positive" chelate effect observed for Et<sub>3</sub>MECAM and enterobactin is solely due to the predisposition of the three chelating arms to bind a metal ion. For the more acidic 3,2-hydroxypyridinonate ligands, both TRENHOPO and hopobactin form a 100-fold weaker ferric complex than the simple bidentate 1-methyl-4-*n*-propylamido-3,2-hydroxypyridinonate model compound (Table 2). By relying on the structural comparison of ferric hopobactin and vanadium(IV) enterobactin, a similar contribution of the triester scaffold toward predisposition of the binding groups is expected for both ligands. Hence, the gain in stability of ferric hopobactin over ferric TRENHOPO is canceled by an antagonistic tethering effect of same magnitude.

Since proton competition for weak acid ligands depends on their relative acidity and pH, the pM value (pM = -log [Fe<sup>3+</sup>]) is a better measure of the relative ligand complexing strength under given conditions ([Fe]<sub>tot</sub> = 10<sup>-6</sup> M, [L]<sub>tot</sub> = 10<sup>-5</sup> M). Calculated pM values at the physiological p[H] of 7.4 for hopobactin, enterobactin, TRENHOPO, and TRENCAM are presented in Table 2. An increase of about 7.2 in the pM value is seen between TRENCAM and enterobactin, whereas the binding affinity of hopobactin increases only by one logarithmic unit when compared with TRENHOPO. At p[H] 7.4, all of the hydroxypyridinonate ligands are nearly fully deprotonated (>90%), so any extra stability would reflect the influence of

the scaffold on metal binding. The p[H] effect on the pM values for the four hexadentate ligands is shown in Figure 12; at low p[H], hopobactin becomes a more effective ligand than enterobactin. The reduced affinity of enterobactin for iron in acidic conditions is due to the basicity of the free ligand and three successive protonation steps of the ferric complex (log K<sub>111</sub> = 4.95, log K<sub>112</sub> = 3.52, and log K<sub>113</sub> = 2.5),<sup>19</sup> the latter resulting in a salicylate mode of binding.<sup>78</sup> For hopobactin no protonation is observed: the complex stays intact and the coordination mode unchanged, even down to p[H] 1.

**Electrochemistry.** Due to the low solubility of the neutral ferric hopobactin complex in water (~10 mM), the cyclic voltammograms were measured in acetonitrile. For comparison, cyclic voltammograms of ferric TRENHOPO were also recorded. Quasireversible signals centered at -782 and -875 mV/0.01 M AgNO<sub>3</sub> are seen for hopobactin and TRENHOPO, respectively. In both cases, the peak separation between the cathodic and anodic waves (ΔE) is 80 mV, and is independent of the sweep rate in the range of 50–200 mV/s. The peak current ratio I<sub>ox</sub>/I<sub>red</sub> is comprised between 0.47 and 0.9 for both complexes. I<sub>ox</sub> and I<sub>red</sub> are both linear functions of the square root of the sweep rate, indicating diffusion limited oxidation and reduction processes. Under the same conditions, ferrocene exhibits similar behavior (ΔE = 75 mV, I<sub>ox</sub>/I<sub>red</sub> = 0.9) with a reduction potential of 91 mV/0.01 M AgNO<sub>3</sub>/Ag.<sup>79</sup>

By relying on extrathermodynamic assumptions discussed by Alexander et al.,<sup>80</sup> the half-wave potential vs NHE in water can be estimated by the formula:<sup>81</sup>

$$E_{\text{NHE}}^{1/2}(\text{H}_2\text{O}) = E_{\text{Ag}^+/\text{Ag}}^{1/2}(\text{S}) + E_{\text{NHE}}^0(\text{Ag}^+, \text{H}_2\text{O}) - \frac{\{\Delta G_{\text{tr}} + RT \ln a_{\text{Ag}^+}\}}{nF} \quad (5)$$

$$= E_{\text{Ag}^+/\text{Ag}}^{1/2}(\text{S}) + 440 \text{ mV}$$

$E_{\text{NHE}}^{1/2}(\text{H}_2\text{O})$ ,  $E_{\text{Ag}^+/\text{Ag}}^{1/2}(\text{S})$ ,  $\Delta G_{\text{tr}}$ , and  $a_{\text{Ag}^+}$  stand for the estimated reduction potential (vs NHE) in water, the measured reduction potential vs the Pleskow electrode in the organic solvent, the free energy change of transfer of Ag<sup>+</sup> from water to the organic solvent, and Ag<sup>+</sup> ion activity in the reference compartment, respectively. The  $\Delta G_{\text{tr}}$  values (-23.2 kJ mol<sup>-1</sup> for acetonitrile) have been tabulated by IUPAC.<sup>82</sup> On the basis of eq 5, estimates of the reduction potentials for ferric hopobactin and TRENHOPO in water are -342 and -435 mV/NHE, which are well within the range of biological reductants and higher than those typically observed for hydroxamate ligands. Ferriochrome A and ferrioxamine B have reduction potentials of  $E^{1/2} = -446$  and  $-454$  mV/NHE, respectively.<sup>83</sup> Noteworthy, TRENHOPO has a higher specificity for iron(III) over iron(II) than hopobactin. The same trend is seen in the high pH limiting reduction potentials of enterobactin<sup>25</sup> and TRENCAM<sup>31</sup> ( $E^{1/2} = -990$  and  $-1040$  mV/NHE, respectively). On the basis of these examples, the triserine ring stabilizes the ferrous over the ferric state compared with the TREN scaffold.

(78) Cass, M. E.; Garrett, T. M.; Raymond, K. N. *J. Am. Chem. Soc.* **1989**, *111*, 1677. Cohen, S. M.; Meyer, M.; Raymond, K. N. Manuscript in preparation.

(79) Diggle, J. W.; Parker, A. J. *Electrochim. Acta* **1973**, *18*, 975.

(80) Alexander, R.; Parker, A. J.; Sharp, J. H.; Waghorne, W. E. *J. Am. Chem. Soc.* **1972**, *94*, 1148.

(81) Gagne, R. R.; Koval, C. A.; Lisensky, G. C. *Inorg. Chem.* **1980**, *19*, 2855.

(82) Marcus, Y. *Pure Appl. Chem.* **1983**, *55*, 977.

(83) Cooper, S. R.; McArdle, J. V.; Raymond, K. N. *Proc. Natl. Acad. Sci. U.S.A.* **1978**, *75*, 3551.

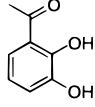
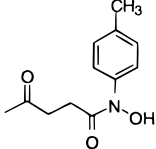
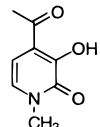
(84) Hou, Z. Ph.D. Dissertation, University of California at Berkeley, 1995.

(85) Ng, C. Y.; Rodgers, S. J.; Raymond, K. N. *Inorg. Chem.* **1989**, *28*, 2062.

(76) Schwarzenbach, G.; Schwarzenbach, K. *Helv. Chim. Acta* **1963**, *46*, 1390.

(77) Carrano, C. J.; Cooper, S. R.; Raymond, K. N. *J. Am. Chem. Soc.* **1979**, *101*, 599.

**Table 2.** Formation Constants and pM Values for Bidentate and Hexadentate Ligands Based on Catecholamides, Hydroxamates and 3,2-Hydroxypyridinonates Binding Groups<sup>a</sup>

R	R'-NH <sub>2</sub>		Hexadentate Ligand		3,2-Hydroxypyridinonate	
	log β <sub>130</sub>	pM	log β <sub>110</sub>	pM	log β <sub>110</sub>	pM
	43.7 <sup>b</sup>	19.7 <sup>b</sup>	43.6 <sup>c</sup>	27.8 <sup>c</sup>	49 <sup>d</sup>	35.5 <sup>d</sup>
	28.3 <sup>e</sup>	13.3 <sup>e</sup>	32.9 <sup>f</sup>	27.8 <sup>f</sup>	no data available	
	28.7 <sup>g</sup>	19.2 <sup>g</sup>	26.7 <sup>h</sup>	26.7 <sup>h</sup>	26.4 <sup>i</sup>	27.4 <sup>i</sup>

<sup>a</sup> pM = -log [Fe<sup>3+</sup>] at p[H] = 7.4 with [Fe]<sub>tot</sub> = 10<sup>-6</sup> M, [L]<sub>tot</sub> = 10<sup>-5</sup> M. <sup>b</sup> R' = C<sub>2</sub>H<sub>5</sub>, ref 84. <sup>c</sup> Reference 31. <sup>d</sup> Reference 19. <sup>e</sup> Acetohydroxamic acid, ref 76. <sup>f</sup> Reference 85. <sup>g</sup> R' = nC<sub>3</sub>H<sub>7</sub>, ref 58. <sup>h</sup> Reference 72. <sup>i</sup> This work.

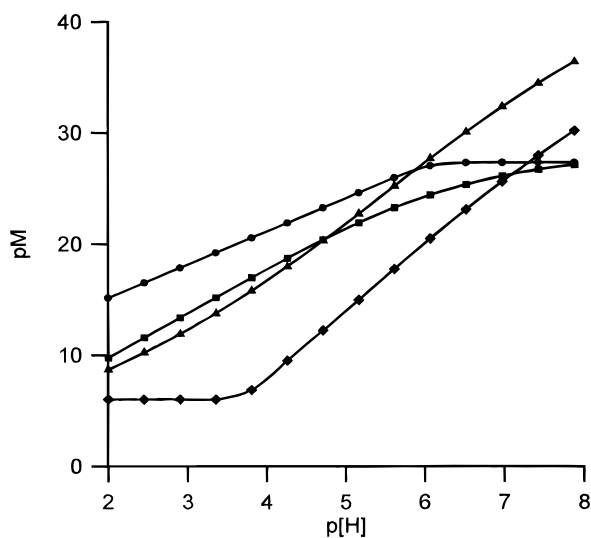


**Figure 12.** Plot of pM vs p[H] for hopobactin (●), TRENHOPO (■), enterobactin (◆) and TRENCAM (▲). [Fe]<sub>tot</sub> = 10<sup>-6</sup> M; [L]<sub>tot</sub> = 10<sup>-5</sup> M.

## Conclusion

A facile method of generating the enterobactin scaffold has been developed. This one-step synthesis of the trityl-protected enterobactin trilactone scaffold gives yields as high as 50%. This synthetic approach enables the development of direct

enterobactin analogs that have appended chelating units other than catecholamides. The 3,2-hydroxypyridinonate derivative, hopobactin, has been synthesized and its iron(III) complex fully characterized. It is the first chiral representative of an iron hydroxypyridinonate complex and under mild acid conditions is the most stable ferric complex known.

Hopobactin and ferric hopobactin provide a good model for studying the structure/function relationships of enterobactin and ferric enterobactin. These and other derivatives, employing hydroxamates, terephthalamides, and salicylates will be examined with respect to their chemical and microbial iron transport properties.

**Acknowledgment.** This paper is dedicated to Professor Dieter Seebach on the occasion of his 60th birthday. This work was supported by NIH Grants AI 11744 and DK32999. The authors thank Dr. F. J. Hollander for assistance with the X-ray diffraction studies and an anonymous reviewer for finding an important numerical error in the stability constants.

**Supporting Information Available:** Table of atomic coordinates and equivalent isotropic displacement parameters, bond lengths and angles, anisotropic displacement parameters, hydrogen coordinates and isotropic displacement parameters for **3** and **8** (21 pages). See any current masthead page for ordering and Internet access instructions.

JA970718N